J Polym Res (2011) 18:1705–1713
DOI 10.1007/s10965-011-9576-8

ORIGINAL PAPER

Synthesis and enhanced swelling properties of a guar gum-based superabsorbent composite by the simultaneous introduction of styrene and attapulgite

Xiaoning Shi · Wenbo Wang · Aiqin Wang

Received: 24 June 2010 / Accepted: 1 February 2011 / Published online: 17 February 2011

Abstract In current study, a series of novel guar gum-*graft*-poly(sodium acrylate-*co*-styrene)/attapulgite (GG-*g*-P(NaA-*co*-St)/APT) superabsorbent nanocomposites were prepared by the simultaneous graft copolymerization of partially neutralized acrylic acid (NaA), styrene (St) and attapulgite (APT) onto natural guar gum (GG), using ammonium persulfate (APS) as the initiator and *N,N′*-methylene-*bis*-acrylamide (MBA) as the crosslinking agent. Fourier Transform Infrared (FTIR) and ultravoilet (UV) spectra confirmed that NaA and St had been grafted onto GG backbones and APT participated in the polymerization reaction. The incorporation of St and APT clearly improved the surface porous morphology of the composites as exhibited by Filed Emission Scanning Electron Microscopy (FESEM). The effect of St and APT on the swelling properties and the swelling kinetics of the developed nanocomposite was investigated. Results showed that the simultaneous incorporation of proper amount of hydrophobic co-monomer St and inorganic nano-scale APT not only obviously enhanced the swelling capacity but highly improved the swelling rate, and the nanocomposite showed better salt-resistant capability and excellent pH-stability in various pH solutions.

Keywords Superabsorbent · Guar gum · Attapulgite · Styrene · Swelling

X. Shi · W. Wang · A. Wang (✉)
Center of Eco-material and Green Chemistry,
Lanzhou Institute of Chemical Physics,
Chinese Academy of Sciences,
Lanzhou 730000, People's Republic of China
e-mail: aqwang@licp.cas.cn

X. Shi
Graduate University of the Chinese Academy of Sciences,
Beijing 100049, People's Republic of China

Introduction

Superabsorbent polymers (SAPs) are three-dimensional physically or chemically crosslinked hydrophilic polymeric materials that can absorb and retain large amounts of water without dissolving and losing their shapes [1]. Owing to the advantageous properties, SAPs have been widely applied in many fields such as agriculture and horticulture [2, 3], sanitary goods [4], wastewater treatment [5, 6], controlled drug delivery systems [7], concrete [8], etc. However, the extension of application domain for SAPs was limited because most of the traditional SAPs are petroleum-based synthetic polymers with high production cost and poor environmental friendly properties [9]. Recently, eco-friendly SAPs have been proposed as "globe-compatible materials" and the design and development about such materials have received considerable attention. Among them, incorporating biodegradable segments as copolymer blocks [10, 11] was taken as the most facile and effective method. Many efforts were made to introduce abundant, renewable, biodegradable, non-toxic and biocompatible natural polysaccharides, such as starch [12, 13], cellulose [14, 15], chitosan [16, 17], sodium alginate [18] and plant gum [19–21] into SAPs for improving their performance and eco-friendly properties. One of the common practices to modify and improve the functional properties of polysaccharides is radical graft copolymerization of vinyl monomers onto the natural polysaccharide, followed by the crosslinking of chains to form three dimensional networks that can swell quickly [22, 23]. Especially, the combination of inorganic clay minerals with the biopolymer network may greatly improve the swelling capacity and decrease the production cost [24, 25].

Guar gum (GG) is a non-ionic natural polymer that consists of polymannan backbone with single galactose unit

side chains. As a low-cost, easily available and non-toxic polysaccharide, GG and its derivatives have been widely applied in many industrial fields [26]. Attapulgite (APT), a kind of naturally occurred nano-scale hydrated octahedral layered magnesium aluminum silicate mineral with exchangeable cations and reactive −OH groups on its surface. Because of its hydrophilic nature and less sensitive to salts comparing with other clays, APT has been more suitable for use in SAPs as additives to improve the water absorption [27].

Recently, it is reported that the introduction of tiny amount of hydrophobic monomer into hydrophilic polymer matrix can alter the physical properties of polymer network and evidently improved the network structure. Because the proper amount of hydrophobic segments may cause a steric repulsion among hydrophilic network, the hydrogen bonding between polymeric chains and the elastic responses of the macromolecular chains in the matrix was decreased, and the swelling capacity and swelling rate can be improved. Many hydrophobic monomers, such as acrylonitrile [28], *N*-butylmethacrylate [29] and styrene [30, 31], have been used as co-monomers for the fabrication of hydrogels. In this paper, based on our previous work on GG-based SAPs [21, 32, 33], appropriate amount of hydrophobic co-monomer St and APT were simultaneously introduced into the GG-*g*-PNaA system to synthesize the eco-friendly guar gum-*g*-poly(sodium acrylate-*co*-styrene)/attapulgite (GG-*g*-P(NaA-*co*-St)/APT) superabsorbent nanocomposite by a facile solution radical polymerization technology. It is expected that the synergistic effect between the hydrophobic phenyl group and APT may further improve the performance of the superabsorbents. The effect of St and APT dosage on the swelling properties of the nanocomposite was investigated to find the optimum synthesis conditions. The chemical structure and surface porous morphology of the nanocomposites were confirmed by FTIR, UV and FESEM techniques, the effect of St and APT on the swelling kinetics and the swelling capacity for optimized nanocomposite in various saline and pH solutions were also investigated.

Experimental

Materials

Guar gum (GG, food grade, M_w=220,000 Da) was obtained from Wuhan Tianyuan Biology Co., China. Acrylic acid (AA) and Styrene (St, chemical pure, Shanghai Wulian Chemical Factory, China), Ammonium persulfate (APS, analytical grade, Xi'an Chemical Reagent Factory, China), *N,N′*-methylene-*bis*-acrylamide (MBA, analytical pure, Shanghai Chemical Reagent Corporation, China), APT micropowder (Gaojiawa Colloidal Co., Jiangsu, China)

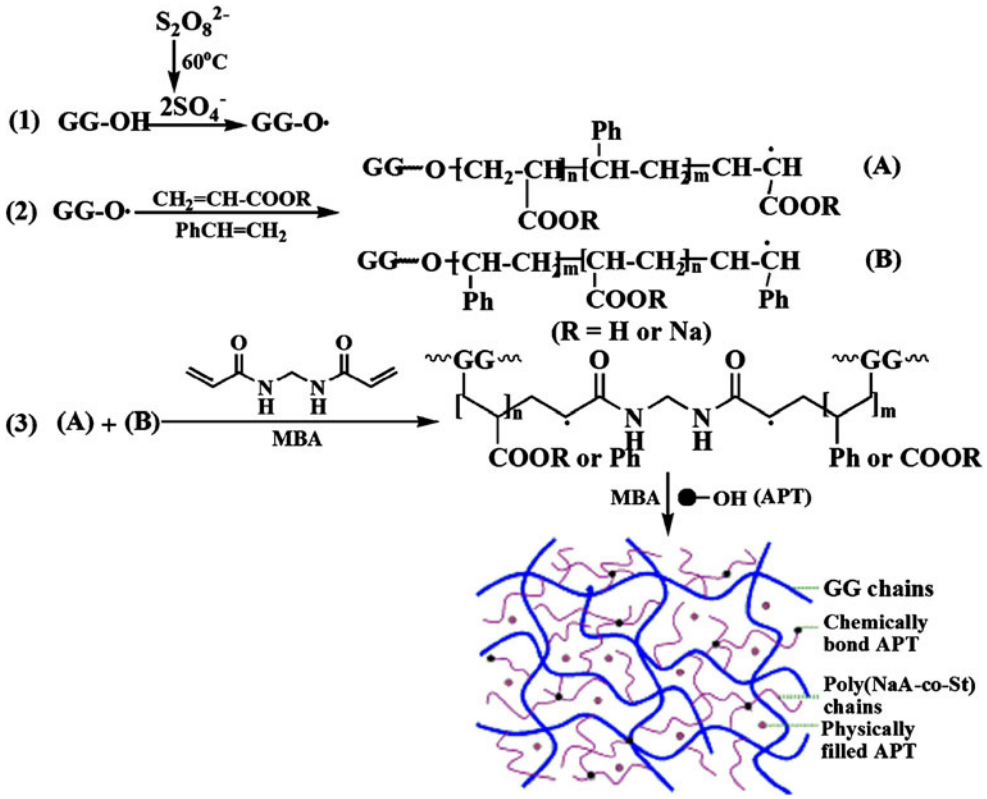

Scheme 1 A proposed reaction mechanism for the formation of GG-*g*-poly(NaA-*co*-St)/APT superabsorbent nanocomposites

was milled and passed through a 200-mesh screen prior to used. Distilled water was used for the preparation and swelling measurement of the samples.

Synthesis of GG-*g*-P(NaA-*co*-St)/APT superabsorbent nanocomposites

GG powder (1.20 g) was dispersed in 34 mL 0.067 M NaOH solution (pH=12.5) in a 250-mL four-necked flask equipped with a mechanical stirrer, a reflux condenser, a thermometer and a nitrogen line. The reactor was immersed in an oil bath at 60°C and kept for 1 h, at the same time, purged with nitrogen to remove the oxygen dissolved from the system. Then, APS (0.10 g, dissolved in 5 mL distilled water) was added to the slurry and the reaction mixture was stirred continuously at 60°C for 10 min. After 10 min, the reactants were cooled to 40°C, a mixture solution composing AA (7.20 g, neutralized by 8.5 mL 8 mol/L NaOH solution), St (0~0.2000 g), MBA (0.0216 g) and certain amount of APT powder was added. Again, the oil bath was gradually heated to 70°C and maintained for 3 h to complete polymerization. Finally, the obtained gel products were washed with distilled water and dried in an oven at 70°C for 72 h. After grinding, the gel particles were passed through 40–80 mesh sieve (180–380 μm).

Measurements of the equilibrium water absorption and swelling kinetics

An accurately weighed sample 0.050 (±0.0001) g (m_1) of the dry powdered superabsorbent with average particle sizes between 180–380 μm was immersed in 250 mL distilled water or 0.9 wt.% NaCl solution for 3 h to reach swelling equilibrium. The swollen gels were filtered through a 100 mesh sieve to remove unabsorbed water for 10 min and weighed (m_2) to obtain the amount of the water absorbed thereby. The equilibrium water absorption (Q_{eq}, g/g) was measured for three times at room temperature according to above method and calculated using the following equation:

$$Q_{eq} = (m_2 - m_1)/m_1 \quad (1)$$

where m_1 and m_2 are the weights of dry and swollen gel, respectively.

The swelling kinetics of the superabsorbents were investigated by monitoring the weight of swollen gels (m_2) at given intervals, such as 1, 3, 5, 7, 10, 15, 20, 30, 60 and 120 min, and the water absorption (Q_t, g·g^{-1}) was calculated using Eq. 1.

Characterization

FTIR spectra were recorded on a Nicolet NEXUS FTIR spectrometer in 4,000–400 cm^{-1} region using KBr pellets. The UV spectra were determined by a UV–vis spectrophotometer (SPECORD 200, Analytik Jera AG), and the

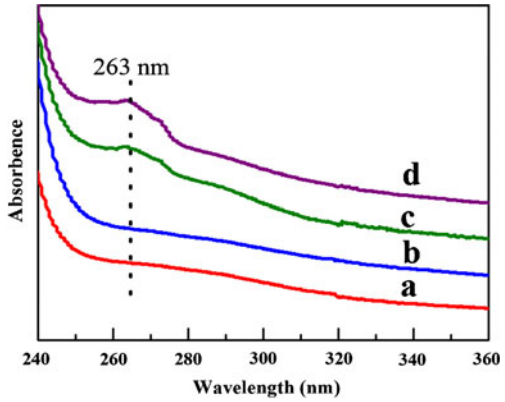

Fig. 2 UV spectra of **a** GG-*g*-PNaA; **b** GG-*g*-PNaA/APT (10 wt.%); **c** and **d** GG-*g*-P(NaA-*co*-St)/APT (C_{St}=24.3, 38.8 mmol/L, respectively; APT, 10 wt.%)

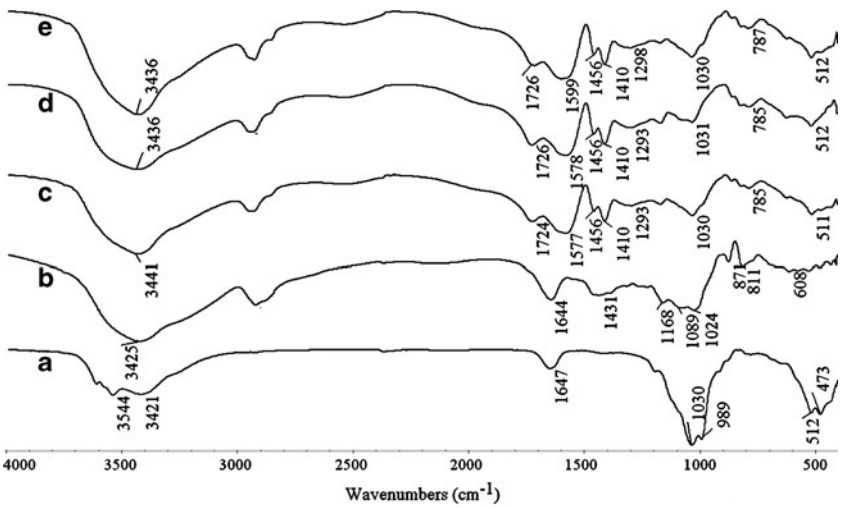

Fig. 1 FTIR spectra of **a** APT, **b** GG, **c** GG-*g*-PNaA/APT, **d** GG-*g*-P(NaA-*co*-St), and **e** GG-*g*-P(NaA-*co*-St)/APT

samples were fully swollen in distilled water. The surface morphologies of the cross-sectioned samples were examined using a JSM-6701F Field Emission Scanning Electron Microscope (JEOL) after coating the sample with gold film.

Results and discussion

Crosslinking and simultaneous graft copolymerization of NaA, St, APT and GG was carried out in the aqueous medium using APS as the radical initiator and MBA as the crosslinking agent. A proposed reaction mechanism was suggested in Scheme 1. First, the thermal decomposition of initiator APS produces sulfates anion radicals [34]. Then the anion radical abstracts hydrogen from the hydroxyl groups of GG backbone and leads to the formation of the corresponding macroradicals. These macroradicals may initiate NaA/St monomers to graft onto GG backbone [35]. At the same time, the crosslinker MBA take part in crosslinking reaction using its vinyl groups. In addition, APT combined with polymeric network through its reactive silanol groups, and thus the three-dimensional network can be regularly formed.

FTIR and UV spectra

FTIR and UV spectroscopy were carried out to reveal the chemical structure of the nanocomposites. Figure 1 shows the FTIR spectra of (a) APT, (b) GG, (c) GG-*g*-PNaA/APT, (d) GG-*g*-P(NaA-*co*-St) and (e) GG-*g*-P(NaA-*co*-St)/APT. It can be noticed that the sharp bands at 3,545 cm^{-1} ascribed to the stretching vibration of the hydrated surface −OH groups of

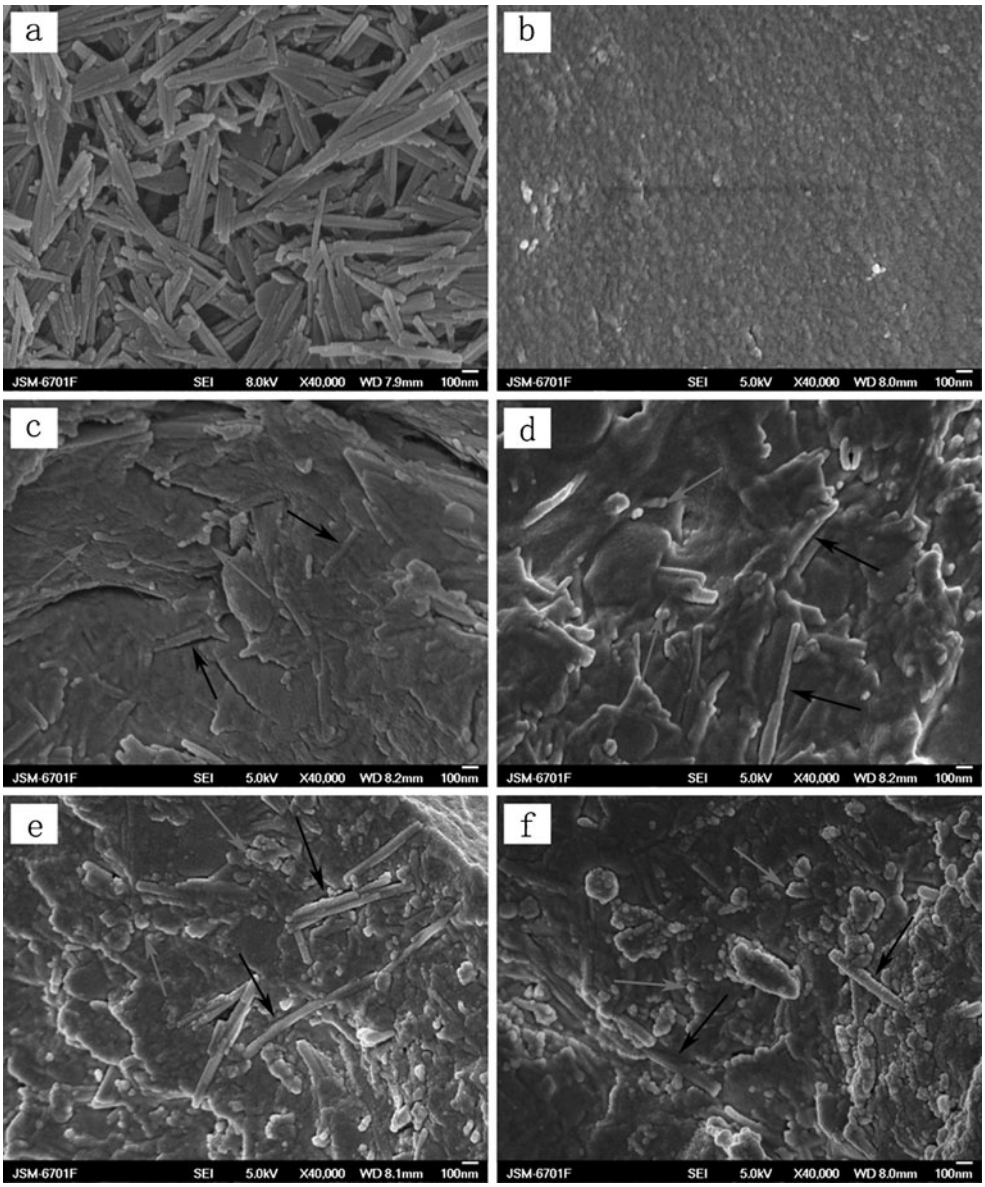

Fig. 3 FESEM photographs of **a** APT and the cross section of **b** GG-*g*-poly(NaA-*co*-St) (C_{St}=24.3 mmol/L); **c** GG-*g*-PNaA/APT (APT 10 wt.%); **d**, **e**, **f** GG-*g*-poly(NaA-*co*-St)/APT (C_{St}=9.7, 24.3, 38.8 mmol/L, respectively; APT, 10 wt.%)

APT disappeared after reaction. Meanwhile, the strong absorption bands at 1,030 cm^{-1} ascribed to −Si–O stretching vibration of APT obviously weaken after reaction, but it can still be observed in the spectra of GG-*g*-PNaA/APT and GG-*g*-P(NaA-*co*-St)/APT (Fig.1a, c, e). This reveals that APT participated in the grafting copolymerization reaction through the surface −OH groups [36]. It can be noted that O–H stretching vibration for GG was obtained at 3,425 cm^{-1}. However, this band was slightly shifted to 3,441 cm^{-1} for the GG-*g*-PNaA/APT composite (Fig. 1c) and to 3,436 cm^{-1} for GG-*g*-P(NaA-*co*-St) and GG-*g*-P(NaA-*co*-St)/APT composite (Fig. 1d, e). It may be attributed to the slight decrease of hydrogen bonding between polymeric chains after the introduction of St [30]. The new absorption bands appeared at 1,726 cm^{-1} and can be assigned to the C = O stretching vibration. The bands around 1,577~1,599 cm^{-1} and 1,410~1,456 cm^{-1} are due to the COO asymmetrical and symmetrical stretching vibration of $-COO^-$ groups, respectively (Fig. 1c–e). Also, the C–OH characteristic absorption of GG at 1,168, 1,089 and 1,024 cm^{-1} was obviously weakened after reaction. This information indicates that the NaA monomer has been grafted onto macromolecular chains of GG. In addition, it was found that there were no obvious difference for the FTIR spectra of GG-*g*-PNaA/APT and GG-*g*-P(NaA-*co*-St)/APT, indicating that the characteristic absorption of St was not conspicuous due to the low dosage of St and was overlapped by the bulk COO^- groups. For proving the existence of St, the UV spectra of the swollen superabsorbents were determined and are shown in Fig. 2. As can be seen, the characteristic peak of St at 263 nm (E band of benzene ring) can be observed in the UV absorption curves of GG-*g*-P(NaA-*co*-St)/APT (C_{St}=24.3, 38.8 mmol/L, respectively; APT, 10 wt.%) in comparison with the curves of GG-*g*-PNaA and GG-*g*-PNaA/APT. This gives direct evidence that St also exists in the polymer network and takes part in graft copolymerization reaction.

Morphological analysis

Figure 3 shows the FESEM photographs of APT and the cross section of GG-*g*-P(NaA-*co*-St) (C_{St}=24.3 mmol/L), GG-*g*-PNaA/APT (10 wt.%) and GG-*g*-P(NaA-*co*-St)/APT (C_{St}=9.7, 24.3, 38.8 mmol/L; APT, 10 wt.%) nanocomposites, which provide a better insight into the dimension and morphology of the nanocomposites. It can be seen from Fig. 3b that GG-*g*-P(NaA-*co*-St) exhibits a comparatively smooth and tight surface, while the nanocomposites incorporated proper amount of APT show a relatively coarse, loose surface and the "lateral" (Fig. 3c~f, black arrow) and "vertical" (Fig. 3c~f, gray arrow) nano-scale APT fibrils were uniformly dispersed in the polymer matrix. Comparing Fig. 3c–f, it was obviously shown that

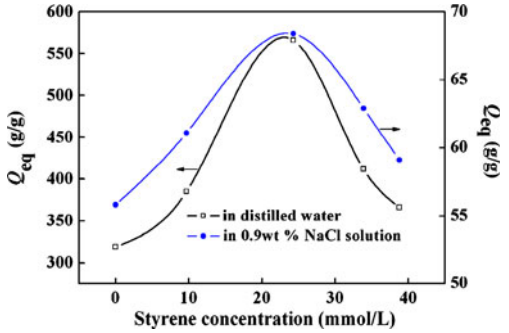

Fig. 4 Effect of St concentration on water absorption (the content of APT in the feed is 10 wt.%)

with increasing the amount of St, the pores on the superabsorbent surface significantly increased. This may be explained by the fact that the existence of hydrophobic St in the hydrophilic polymer matrix can form hydrophobic micro-domains [37] or relax the physical forces by decreasing the hydrogen bonding between polymeric chains [30]; all these could expand the mesh size. But too much hydrophobic groups often reduce hydration degree of the superabsorbent. According to the above observation from FESEM, the amount of hydrophobic monomer St and APT have great influence on the micro-surface structure of the nanocomposites and also affect the swelling properties of the superabsorbent. Thus, the swelling behaviors of nanocomposite including different dosage St and APT samples were investigated as follows.

Effect of St concentration on water absorption

The introduction of hydrophobic monomer into the hydrophilic system was taken an effective route to improve the absorption property [30, 37]. In this section, the effect of St concentration on the swelling capacity of the superabsorbent was investigated by varying St concentration from 0 to 38.8 mmol/L (Fig. 4). It can be noticed that the equilibrium water absorption drastically increases with increasing the proportion of St from 0 to 24.3 mmol/L, reached a

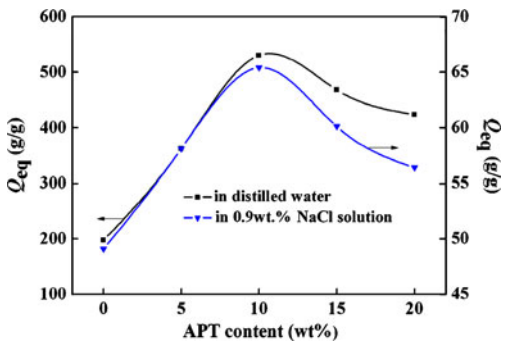

Fig. 5 Effect of APT content on water absorption (the St concentration in the feed is 24.3 mmol/L)

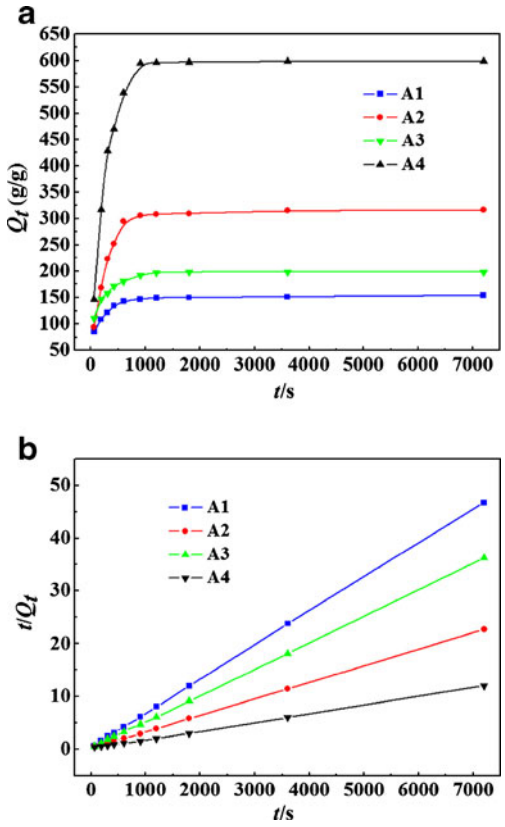

Fig. 6 Effect of St and APT on the swelling kinetics

maximum at 24.3 mmol/L and then decreased with the further increase of St concentration. The observed initial increase in the water absorption may be attracted to the fact that there are many hydrogen bonds between hydrophilic −OH and −COOH groups of the superabsorbent, which can act as physical crosslinking points in the nanocomposite network. It is well known that with the increase of crosslinking points, the swelling decreases. So, the presence of hydrophobic phenyl rings as pendant groups causes a steric repulsion among networks, which widen the mesh size of the network pores and thus decreases the hydrogen bonding between polymeric chains. As a result, the water molecules can penetrate into the superabsorbent network more easily, and the water absorption was evidently enhanced. However, the inclusion of a hydrophobic monomer in the gel matrix often lead to the decreased hydration degree of the gel [31], which is responsible for the shrinkage of water absorption. Thus, beyond the optimum St concentration (24.3 mmol/L), the equilibrium absorption obviously decreases.

Effect of APT content on water absorption

Clay content is an important factor affecting water absorption of the organic–inorganic superabsorbent composite [32]. The influence of the amount of APT in the nanocomposite on the water absorption was investigated and the results are shown in Fig. 5. It can be seen that the water absorption of the nanocomposite was increased to 530 g/g in distilled water and 65 g/g in 0.9 wt.% NaCl solution with increasing the APT content to 10 wt.%, and then decreased with the further increase of APT. As described by Haraguchi [38], the inorganic clay particles in the polymer network act as an additional network point. Appropriate amount of −OH on the surface of APT could react with NaA, which could improve the polymeric network and then enhance the equilibrium water absorption. However, further increasing the APT content may result in the generation of more crosslink points and the increase of crosslinking density, and then the expansion of polymer network was restricted. Additionally, excess APT only acts as filler and the amount of hydrophilic groups in the unit composites decreases with the increase of APT content. All these resulted in a decrease in the water absorption. Meanwhile, APT is a kind of salt resistant clay, and the introduction of APT into the polymeric network results in the generation of a salt resistant superabsorbent composite. Compared with clay-free superabsorbent, Fig. 5 also shows that the superabsorbent nanocomposite had a high water absorption capacity of 424 g/g in distilled water and 56 g/g in 0.9 wt.% NaCl solution, even the content of APT reached 20 wt.%. This is favorable to improve the salt-resistant properties and reduce the production cost.

Effect of St and APT on swelling kinetics

The effect of St and APT on swelling kinetics for GG-based SPAs were measured and plotted in Fig. 6a. For the kinetic analysis, the Schott's second-order swelling kinetic model [39] was utilized.

$$t/Q_t = 1/K_{\mathrm{is}} + 1/Q_{\infty} t \qquad (2)$$

Where, Q_t is the water absorption at a given time t; K_{is} is the initial swelling rate constant ($g \cdot g^{-1} \cdot s^{-1}$); Q_{∞} ($g \cdot g^{-1}$) is

Table 1 Equilibrium water absorbency and swelling kinetic parameters of the GG-*g*-poly (NaA-*co*-St)/APT superabsorbents

Samples	Q_{eq} (g/g)	Q_{∞} (g/g)	K_{is} (g/g/s)	R
St, 0 mmol/L; APT, 0 wt.% (A1)	154	155	2.4971	0.9999
St, 0 mmol/L; APT, 10 wt.% (A2)	316	323	3.2147	0.9998
St, 24.3 mmol/L; APT, 0 wt.% (A3)	199	201	3.8342	0.9999
St, 24.3 mmol/L; APT, 10 wt.% (A4)	599	610	6.0394	0.9997

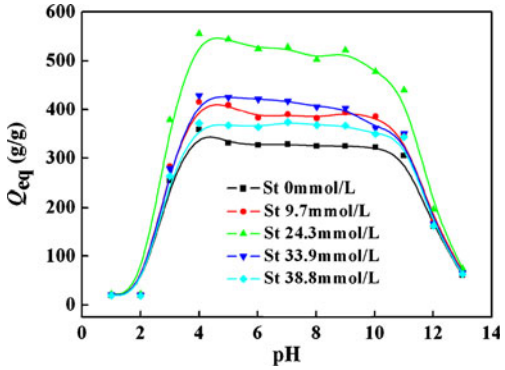

Fig. 7 Effect of external pHs on the water absorption of the superabsorbent nanocomposites with different St concentration (APT, 10 wt.%)

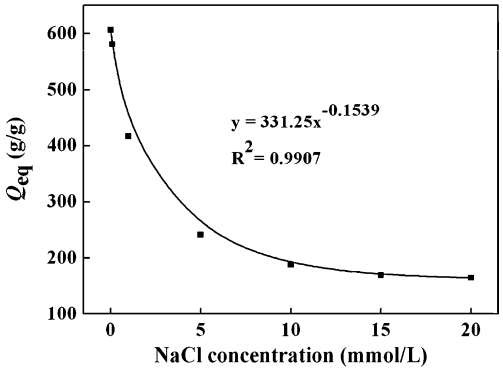

Fig. 9 Swelling capacity variation of the optimized nanocomposite in NaCl solution with various concentrations

the theoretical equilibrium water absorption ($g \cdot g^{-1}$). According to the results shown in Fig. 6a, the plots of t/Q_t vs. t give straight lines with good linear correlation coefficient R>0.999 (Fig. 6b) and it is possible to model the swelling kinetics of the nanocomposites with the above mentioned Eq. 2 and to determine the values of the swelling kinetics parameters, Q_∞ and k_{is}, from the slopes and intercepts of these straight lines. The obtained values for the swelling kinetics parameters are presented in Table 1. It can be seen that the initial swelling rate constant (K_{is}) of the GG-based SAPs is markedly increased by the simultaneous introduction of 24.3 mmol/L St and 10 wt.% APT. As reported [11], the incorporation of inorganic clay may reduce the entangling of polymer chains. However, APT is rigid and distributed in the polymer network at nanoscale particles. Different from this, the hydrophobic polystyrene chain segments are flexible. Thus, the introduction of proper amount of St might decrease the defects resulting from the rigid APT, and the synergistic effects of APT and St on the polymer network which contributed to decrease physical crosslinking and improve the swelling rate.

Effect of external pH on water absorption

The role of pH in regulating water absorption of polymeric hydrogels is of greater significance as a change in pH of the swelling medium. In the present investigation, the water absorption of the superabsorbent with different St and APT dosages was studied at various pH solutions range from 1.0 to 13.0. Figures 7 and 8 demonstrates the swelling behaviors of the superabsorbents with different St concentration (the weight content of APT was fixed at 10 wt.%) and different APT weight contents (the concentration of St was fixed at 24.3 mmol/L) in various pH solutions. By comparing the swelling curves shown in Figs. 7 and 8, it can be seen that the change in external pH have an similar effect on the swelling behavior of each superabsorbent. This is because that the synergistic effect of St segment and APT in gel network decreased the physical crosslinking degree. The absorption of all samples increased sharply as the pH increased from 2 to 4 and then drastically decreased in the pH range of 10~13. This behavior may be explained as follows: in acidic pH solution (<4), the $-COO^-$ group on the polymeric chain can turn into −COOH group (the pKa of acrylic acid is 5.4), most of the $-COO^-$ anions were

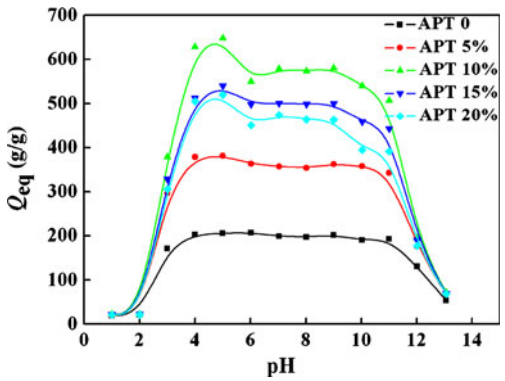

Fig. 8 Effect of external pHs on the water absorption of the superabsorbent nanocomposites with different APT content (C_{St}= 24.3 mmol/L)

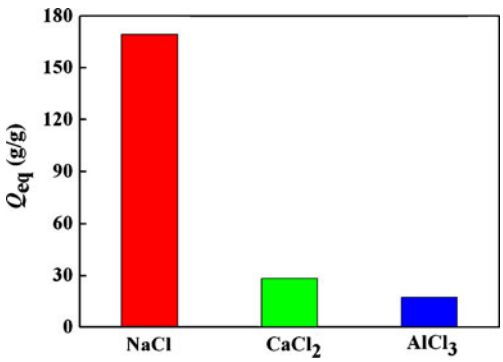

Fig. 10 Swelling capacity of the optimized nanocomposite in salt solutions of different valence (0.15M)

protonated. So, the main anion–anion repulsive forces were eliminated, which induced almost nil osmotic swelling pressure and consequently the swelling values were decreased. At higher pH values (5–9), some of $-COO^-$ groups were ionized and the electrostatic repulsion between $-COO^-$ groups causes an enhancement of the swelling capacity. Again, a charge screening effect of the counter ions (cations) limits the swelling at pH >10. Similar swelling-pH dependencies have been reported in the case of other superabsorbent systems [40, 41].

Effect of salt solution on the swelling properties

Swelling capacity in salt solution has prime significance for the practical applications of superabsorbents such as personal hygiene products and agriculture. In the present study, the swelling capacity of the optimized sample was studied in saline solutions with various concentrations (Figs. 9 and 10). It is obvious that the swelling of the superabsorbent in saline solution was appreciably decreased compared to that in distilled water. This well-known undesired swelling-loss is often attributed to a "charge screening effect" of the additional cations, which causes a non-perfect anion-anion electrostatic repulsion and causes a decreased osmotic pressure difference between the hydrogel network and the external solution. In addition, in the case of multivalent salt solutions, "ionic crosslinking" at the surface of particles causes an appreciably decrease in swelling capacity. There is a law relation between the swelling capability and the concentration of a salt solution [42]:

$$\text{Swelling} = k[\text{salt}]^{-n} \quad (3)$$

where k and n are constant values for an individual superabsorbent; k value is swelling at a high concentration of salt and n value is a measure of salt sensitivity. Figure 10 indicates that increasing the salt concentrations (>0.2M) has no appreciable influence on the water absorption of the superabsorbent. From Fig. 10, it can be seen that the water absorption for the superabsorbent in the multivalent saline solutions is the order of monovalent > divalent > trivalent cations. Here, the effect of the ionic crosslinking produces more effective factor against swelling rather than the charge screening effect of the cations.

Conclusions

A novel biopolymer-based superabsorbent nanocomposite based on natural GG was firstly prepared by radical graft copolymerization of NaA and St in aqueous solution using *N,N′*-methylene-*bis*-acrylamide as a crosslinking agent and ammonium persulfate as an initiator. APT was used as inorganic nano-scale additives.

FTIR and UV spectroscopy were used to confirm the structure of the developed nanocomposites. The effect of St and APT dosage in polymer matrix on the swelling behavior was investigated. The results indicated that the variation in St and APT dosage in the feed mixture of the superabsorbent brings about an increase in water absorption capacity, while beyond the optimized dosage of St and APT, the added components often induced a reduction of the swelling capacity. The simultaneous introduction of proper amount of hydrophobic St monomer and APT clay into the GG-*g*-PNaA matrix contributed to improve the physical properties and the three-dimensional network of the nanocomposite, and enhance the swelling properties. The maximum water absorption (566 g/g) was achieved under the optimum reaction conditions: the weight ratio of GG to AA=1 : 6, C_{St}= 24.3 mmol/L, weight content of APT=10 wt.%, C_{APS}= 8.9 mmol/L, C_{MBA}=2.8 mmol/L. The effect of St and APT on swelling kinetics was also measured and the synergistic effect of St and APT could highly improve the swelling rate of the superabsorbent nanocomposites. Swelling measurements in different pH solutions and different salt solutions indicated that the superabsorbent nanocomposites have appreciable pH-stability and salt-resistant property, which can be used as a suitable candidate for applications in agriculture and horticulture. Furthermore, the superabsorbent nanocomposites based on natural resources and inorganic clay mineral were quite eco-friendly and cost-efficient.

Acknowledgments This work was financially supported by "863" Project of the Ministry of Science and Technology, P. R. China (No. 2006AA03Z0454 and 2006AA100215).

References

1. Buchholz FL, Graham AT (1998) Modern superabsorbent polymer technology. Wiley-VCH, New York, Chap. 1–7
2. Teodorescu M, Lungu A, Stanescu PO, Neamtu C (2009) Ind Eng Chem Res 48:6527–6534
3. Zhao GZ, Liu YQ, Tian Y, Sun YY, Cao Y (2010) J Polym Res 17:119–125
4. Kosemund K, Schlatter H, Ochsenhirt JL, Krause EL, Marsman DS, Erasala GN (2009) Regul Toxicol Pharmacol 53:81–89
5. Kaşgöz H, Durmus A (2008) Polym Adv Technol 19:838–845
6. Güçlü G, Keleş S, Güçlü K (2006) Polym Plast Technol Eng 45:55–59
7. Sadeghi M, Hosseinzadeh HJ (2008) J Bioact Compat Polym 23:381–404
8. Jensen OM, Hansen PF (2001) Cem Concr Res 31:647–654
9. Kiatkamjornwong S, Mongkolsawat K, Sonsuk M (2002) Polymer 43:3915–3924
10. Li W, Wang JL, Zou LZ, Zhu SQ (2008) J Polym Res 15:435–445
11. Hwang DC, Damodaran S (1997) J Am Oil Chem Soc 74:1165–1171

12. Al E, Güçlü G, İyim TB, Emik S, Özgümüs S (2008) J Appl Polym Sci 109:16–22
13. Sadeghi M, Hosseinzadeh H (2008) TUrk J Chem 32:375–388
14. Demitri C, Sole RD, Scalera F, Sannino A, Vasapollo G, Maffezzoli A, Ambrosio L, Nicolais L (2008) J Appl Polym Sci 110:2453–2460
15. Pourjavadi A, Ghasemzadeh H, Mojahedi F (2009) J Appl Polym Sci 113:3442–3449
16. Xie YT, Wang AQ (2009) J Polym Res 16:143–150
17. Chen Y, Liu YF, Tan HM, Jiang JX (2009) Carbohydr Polym 75:287–292
18. Hua SB, Wang AQ (2009) Carbohydr Polym 75:79–84
19. Pourjavadi A, Sadeghi M, Hosseinzadeh H (2004) Polym Adv Technol 15:645–653
20. Mohamadnia Z, Zohuriaan-Mehr MJ, Kabiri K, Razavi-Nouri M (2008) J Polym Res 15:173–180
21. Wang WB, Zhang JP, Wang AQ (2009) Appl Clay Sci 46:21–26
22. Bardajee GR, Pourjavadi A, Sheikh N, Amini-Fazl MS (2008) Radiat Phys Chem 77:131–137
23. Hennink WE, van Nostrum CF (2002) Adv Drug Deliv Rev 54:13–36
24. Wu JH, Lin JM, Zhou M, Wei CR (2000) Macromol Rapid Commun 21:1032–1034
25. Lee WF, Chen YC (2005) J Appl Polym Sci 97:855–861
26. Soppirnath KS, Aminabhavi TM (2002) Eur J Pharm Biopharm 53:87–98
27. Li A, Zhang JP, Wang AQ (2007) J Appl Polym Sci 105(6):3476–3482
28. Lee WF, Yeh YC (2005) Eur Polym J 41:2488–2495
29. Shukla S, Bajpai AK, Kulkarni RA (2005) J Appl Polym Sci 95:1129–1142
30. Marandi GB, Hariri S, Mahdavinia GR (2009) Polym Int 58:227–235
31. Tang C, Ye S, Liu H (2007) Polymer 48:4482–4491
32. Wang WB, Zheng YA, Wang AQ (2008) Polym Adv Technol 19:1852–1859
33. Wang WB, Wang AQ (2009) Carbohydr Polym 77:891–897
34. Yoshida T, Hattori K, Sawada Y, Choi Y, Uryuz T (1996) J Polym Sci A Polym Chem 34:3053–3060
35. Taunk K, Behari K (2000) J Appl Polym Sci 77:39–44
36. Li A, Wang AQ, Chen JM (2004) J Appl Polym Sci 92:1596–1603
37. Bajpai AK, Shrivastava M (2002) J Macromol Sci Pure Appl Chem 39:667–692
38. Haraguchi K, Takehisa T (2002) Adv Mater 14:1120–1126
39. Schott H (1992) J Pharm Sci 81:467–470
40. Pourjavadi A, Kurdtabar M, Mahdavinia GR, Hosseinzadeh H (2006) Polym Bull 57:813–824
41. Pourjavadi A, Amini-Fazl MS, Hosseinzadeh H (2005) Macromol Res 13:45–53
42. Bajpai AK, Shrivastava M (2000) J Macromol Sci Pure Appl Chem 37:1069–1088